2023 IEEE International Conference on Communications, Control, and Computing Technologies for Smart Grids (SmartGridComm) | 978-1-6654-5556-5/23/$31.00 ©2023 IEEE | DOI: 10.1109/SmartGridComm57358.2023.10333918

Network Performance Analysis of Smart Grid Communications Over LTE cat-M[1]

Biswajit Kumar Dash*, Sureel Shah**, and Filippo Malandra*

*Department of Electrical Engineering, State University of New York at Buffalo, NY, USA
**Department of Electrical and Computer Engineering, University of California, San Diego, CA, USA

***Abstract*—Smart grid applications heavily rely on communication infrastructures that offer flexibility, scalability, and cost-effectiveness to enable bi-directional information exchange across geographically distributed grid elements. Wireless cellular networks, such as LTE cat-M, provide extensive coverage at a reduced cost, both in terms of installation and power consumption. This paper presents a multi-node testbed to assess the suitability of LTE cat-M technology for a variety of smart grid applications, with distributed nodes collecting and transmitting data at a variable rate, from 0.25 to 100 frames per second (fps). Based on field experiments, an extensive performance analysis is presented with Key Performance Indicators (KPIs), such as delay, jitter, and frame loss. The impact of the number of smart grid nodes and propagation quality are also considered in the analysis. Finally, a calibration method to optimize the packet transmission time is presented with a 33.91% delay reduction under different conditions.**

***Index Terms*—Smart Grid communications, LTE Cat-M, Cellular-IoT, Network performance, Multi-node testbed**

I. Introduction

Emerging and future smart grid applications are becoming increasingly reliant on communication and networking technologies to overcome the power system scale requirements and inherent heterogeneity. Ever-increasing reliability, reduced latency, and scalable connectivity options are necessary for integrating interconnected grid elements to provide timely and bi-directional information exchange across the geographically distributed areas of the power grid.

The advancement of wired and wireless communication, coupled with the interoperability of Internet of Things (IoT) devices, has enabled intelligent monitoring and management capabilities of distributed power systems, fostering more efficient smart grid operations. Traditional grid infrastructures often rely on wired networks like Ethernet, fiber optic communication, or Power Line Communication (PLC), given their robust performance, low transmission latency, and immunity to interference [1]. However, modern smart grids necessitate more flexible, scalable, and cost-effective communication solutions that seamlessly integrate a diverse array of devices and renewable energy sources, making wireless communication technologies an increasingly preferred choice [2]. A significant portion of previous research primarily focused on the application of cellular and broadband wireless technologies, including microwave and satellite [3], WiMAX [4], UMTS [5], 3G, and LTE [6], [7].

[1]This material is based upon work supported by the National Science Foundation under Grant No. 2105230.

However, these technologies are predominantly broadband and, despite their high performance and low delay, are not particularly suitable for the integration of a large number of simple devices, such as sensors, smart meters, and micro Phasor Measurement Units (μ-PMUs), which transmit a small amount of data at a variable rate. The need for smart, cost-effective, and efficient solutions to interconnect these devices has pushed research to explore the use of predominantly IoT technologies, such as LTE cat-M [8]. Among the advantages of LTE cat-M networks, we can list their power-saving mode, limited frequency spectrum usage, and low-cost radios and data plans (compared to conventional LTE networks). However, to assess their suitability to support the highly diverse smart grid traffic, accurate network analyses are needed.

In our prior work [9], we investigated the network performance of LTE cat-M, with a particular focus on communications in a smart grid environment. However, we mainly focused on the design and performance analysis of a single Arduino-based smart grid node. In this work, we extend the performance analysis in [9] by considering multiple smart grid nodes that communicate wirelessly using LTE cat-M technology. The multi-node feature permits analyzing the interplay among nodes in a real smart grid environment. By undertaking a series of thorough experiments, we aim to provide a more realistic assessment of LTE cat-M's suitability for smart grid communications. Through this, we are furthering the understanding of this technology's potential and limitations, laying the groundwork for its application in current and future smart grid deployments. The main contributions of this paper are: i) detailed performance analysis based on network Key Performance Indicators (KPIs) such as delay, jitter, and frame loss; ii) analysis of the influence of signal quality metrics on network performance; iii) analysis of different reporting rates and indoor/outdoor differences; and iv) a novel approach to reduce the delay by opportunistically selecting the best time for smart grid nodes to start their data transmission.

The remainder of this paper is organized as follows: in Section II, an overview of the state of the art is described; in Section III, the architecture of our testbed is described; in Section IV, experimental results are reported; in Section V, the conclusions are discussed.

II. State of the Art

Various studies have underscored the integral role of communication networks in modern smart grids [10], [11]. The

robustness of these networks is key to smooth grid operations, interoperability among various components of the smart grid, quality service for grid applications, and secure power generation, transmission, and distribution. The envisioned communication solutions must cope with the demanding needs of current and future applications, such as ultra-low delay in grid protection and control [10], [11].

However, a thorough network performance analysis is paramount to ensure these smart-grid constraints are satisfied. Current approaches to network performance analysis in a smart grid environment are based on stochastic simulations, mathematical analysis, and experimental testbeds, each providing unique insights. A recent survey has highlighted the current state-of-the-art performance evaluation methodologies and emphasized the need for a co-simulation-based evaluation framework for substation automation design [12]. Research has also unveiled tools to analyze large-scale RF-Mesh-based wireless networks [13] and data-driven methods for controlling Distributed Energy Resources (DER) [14]. While simulations and analytical methods can be cost-effective by predicting communication network behavior in the design phase, experimental analyses offer tangible insights into the complexities of smart grid communication systems. For instance, the efficacy of a communication platform using PLC and optical fiber has been validated through a field trial in a real distribution network and further assessed via simulation-based experiments to facilitate real-time state estimation via PMUs [15]. Another study has highlighted the effectiveness of PLC in advanced smart grid control systems, as evidenced by successful field trials and pilot projects [16].

To fully leverage smart grid systems, both wired and wireless network solutions are employed. Despite wired networks' stability and performance benefits, wireless solutions are gaining popularity for their ease of installation, scalability, and lower costs [2]. Wireless solutions, like WiMAX and Wireless Local Area Networks (WLANs), have shown their potential in distribution area networks within smart grids [4] and distributed generation grids [17]. Moreover, a hybrid wireless system using WiFi and WiMAX has proven its worth in power line monitoring [18]. However, their coverage limitations have led to exploring alternatives like LTE.

The LTE technology holds significant potential for enhancing smart grid communications and applications. For instance, the potential of a realistic LTE network to support smart grid traffic in a smart city has been analyzed in [7]. However, this study focused solely on Machine-to-machine (M2M) traffic [7]; others considered both human and M2M traffic [19], [20]. Moreover, advancements in IoT technology, such as Zigbee and cloud-based systems, have contributed significantly to power management strategies and distribution networks [21], [22]. Despite their potential, both traditional LTE and Zigbee have limitations when applied to large-scale smart grids: the former is not optimized to transmit small sensor data (due to a heavy protocol's overhead) [23], and the latter lacks reliability, especially in harsh environments where multiple wireless technologies coexist [24].

In response to these challenges, Cellular-IoT (C-IoT) networks have been proposed and, in particular, are able to provide significant coverage enhancements over traditional LTE systems and reduce equipment costs [25]. The study in [26] offers insights into the features and challenges of C-IoT networks such as LTE Cat-M and Narrowband IoT (NB-IoT). The LTE cat-M-based performance analysis presented in our prior work [9] has further demonstrated the potential of this wireless technology to support smart grid communication systems. That paper mainly focused on the implementation design and performance analysis of a single smart grid node (i.e., an Arduino-based μ-PMU) with a brief discussion on multi-node performance. However, as multi-node synchrophasor systems are becoming increasingly valuable in the development and operation of modern smart grids [2], our study leverages our proprietary testbed (consisting of eight Arduino-based smart grid nodes within a commercial LTE cat-M network) to provide a comprehensive performance analysis of a variety of multi-node smart grid networks.

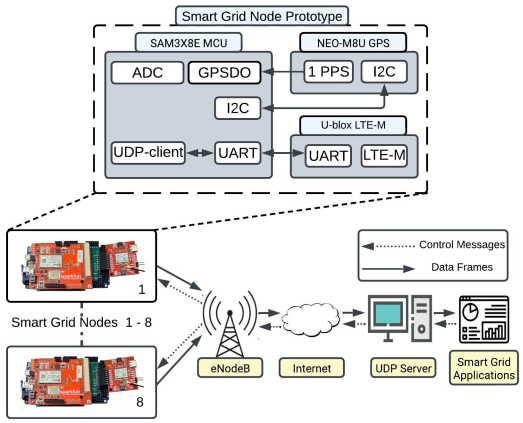

Figure 1: LTE-M based multi-node smart-grid communication system.

III. System Description

In this section, we present the single-node design (Section III-A) and then provide details on the architecture of our multi-node testbed (Section III-B).

A. Single node implementation

The system schematic of our smart grid node prototype is shown in the upper section of Fig. 1. This design modifies the prototype proposed in our prior work [9], where a smart grid node consisted of a communication module and a data frame generation module. Each module required a separate Microcontroller Unit (MCU), resulting in additional complexity, delays, and energy consumption. In the current work, as shown in Fig. 1, we have improved the design by using a single Arduino DUE, capable of generating as well as transmitting synchronous smart grid data.

The Arduino DUE dev. kit, which consists of the Atmel SAM3X8E ARM Cortex-M3 CPU, forms the computational backbone of the prototype, and its Analog-to-digital Converter (ADC) unit can be used to sample the power signal and compute, for instance, synchrophasor data frames following the

IEEE C37.118.2 synchrophasor standard [27]. However, this research focuses mainly on the communication performance of a generic smart grid application; therefore, further details on the synchrophasor application are not provided.

B. Architecture of the proposed multi-node testbed

The proposed multi-node testbed, depicted in Fig. 1, comprises eight smart grid nodes connected to an LTE base station (eNodeB) and reports data to a single UDP server (hosted in the University at Buffalo), whose data can be accessed by a generic smart grid application manager.

As shown in Fig. 1, there are two types of transmissions: i) control messages and ii) data frames. Control messages are transmitted by the server to configure smart grid nodes and shape their communication traffic (e.g., packet size, transmission rate, start time, and duration of each transmission). These parameters can be tuned to represent various smart grid applications, such as PMUs, smart metering, and state estimation. On the other hand, data frames are generated from each smart grid node and are transmitted at various rates to the UDP server.

IV. Numerical results and end-to-end delay analysis

In order to assess the suitability of LTE cat-M for smart grid applications, we conducted a number of experiments to measure and analyze the performance of such technology when transmitting smart grid traffic. Network Time Protocol (NTP) was used to maintain the eight smart grid nodes in the network synchronous with the UDP server. The high accuracy of NTP is fundamental in analyzing the frame delay, which was computed as the received time (at the UDP server) minus the generation time (timestamped at the smart grid node) of each frame.

Each smart grid node *periodically* transmits data frames at a rate of λ frames per second (fps). This assumption can accommodate a wide variety of smart grid data, such as synchrophasors or smart metering. A detailed end-to-end network performance analysis is carried out, considering KPIs, such as delay, jitter, and frame loss. As observed in [9], the delay (and network performance in general) is mainly affected by LTE cat-M.

To dive deep into the performance of LTE cat-M, we have conducted a number of experiments, including indoor vs. outdoor comparison (Section IV-A), LTE signal quality vs. performance (Section IV-B), the impact of the number of nodes (Section IV-C), transmission start time optimization (Section IV-D), and analysis of different smart grid applications (Section IV-E). Each experiment spanned around 5 minutes. It is worth noting an initial burst of frame loss was observed during our experiments, likely due to the startup of the Arduino and the time needed to establish LTE cat-M connectivity successfully. We addressed this issue by excluding the first 50 frames from the analysis.

A. Overview of the outdoor and indoor experimental results

To evaluate the performance of LTE cat-M technology in diverse environments, we conducted a series of indoor and outdoor experiments, detailed in this section. The experiments encompassed four smart grid nodes transmitting 15000 frames each at a rate of λ = 50 fps over 300 seconds. Key metrics such as delay (minima, maxima, mean, standard deviation (St.d.), and 95% Confidence Interval (95% CI)), jitter, and frame loss were examined. Table I presents a summary of our findings.

Table I: Multi-node delay statistics and frame loss in outdoor and indoor experiments.

Node ID.	Delay (ms)								
	Min	Max	Mean	St.d.	Q1	Q3	Jitter	95% CI	Loss(%)
Outdoor									
1	140.02	445.13	176.44	19.11	161.28	190.12	18.35	176.44 ± 0.31	1.29
2	142.94	376.24	177.23	17.47	162.77	189.29	18.19	177.23 ± 0.28	1.16
3	139.37	356.39	176.42	18.10	161.48	188.58	18.51	176.42 ± 0.29	1.08
4	142.31	330.67	176.11	17.32	162.38	186.96	17.42	176.11 ± 0.28	0.98
Indoor									
1	141.87	1102.67	196.36	79.10	164.91	200.30	18.82	196.36 ± 1.27	1.48
2	143.83	1173.68	202.69	78.36	172.32	206.50	18.82	202.69 ± 1.27	1.52
3	143.63	1065.59	199.34	80.06	167.33	200.87	18.49	199.34 ± 1.28	0.97
4	141.54	1146.93	205.41	88.94	167.07	203.15	18.17	205.41 ± 1.44	1.32

In the outdoor environment, we observed a closely uniform mean transmission delay across all nodes, ranging from 176.11 ms (node 4) to 177.23 ms (node 2). Transmission stability, as reflected by the jitter values, also showed consistency, ranging narrowly from 17.42 ms (node 4) to 18.51 ms (node 3). Likewise, other metrics indicating the variability in transmission delays, specifically St.d. and 95% CI of the mean delay, demonstrated uniform distribution among the nodes. Despite the uniform delay metrics, frame loss exhibited variation across nodes, from 0.98% (node 4) to 1.29% (node 1).

An analysis of the indoor experimental results, despite a small variation in mean delay values between 196.36 ms (node 1) and 205.41 ms (node 4), revealed larger delays with respect to outdoor transmissions (the average indoor delay is 13.82% higher than outdoor). Despite these variations, the small 95% CIs suggest lower uncertainty in the experiments. However, frame loss rates exhibited minor performance variability, ranging from 0.97% to 1.52%. Interestingly, jitter values remained consistent across all nodes, indicating a stable quality of service despite the variations in delay and frame loss.

To further compare the network performance in indoor/outdoor environments, we have analyzed the time series of the delays, which are visualized in Fig. 2. In both outdoor and indoor experiments, most frames display a delay between approximately 150 to 200 ms. However, a number of "narrow delay peaks" are observed in indoor settings. These peaks are most likely due to network degradation phenomena, such as multipath fading, interference, and obstructions. These effects largely impacted indoor propagation, leading to a larger mean delay (+13.82%) and frame losses (+17.29%). However, despite these minor variations, the overall performance of the LTE Cat M network remained robust across both settings, underscoring the resilience of our custom-built nodes to maintain acceptable performance under diverse conditions.

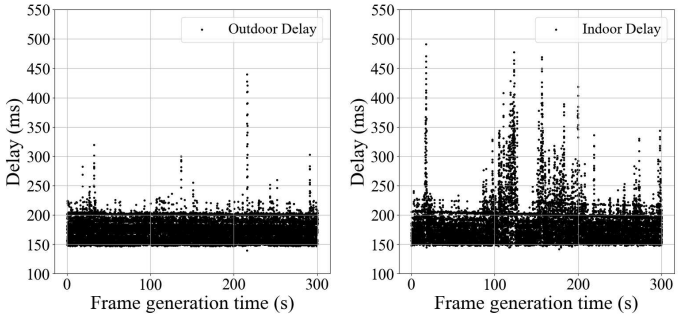

Figure 2: Delay variation over time for outdoor and indoor experiments.

B. LTE signal quality metric Vs performance

In this study, we have analyzed the impact of signal quality metrics, such as Reference Signal Received Power (RSRP), on network performance in nine distinct locations. We averaged the results from experiments conducted at a transmission rate of $\lambda = 50$ fps.

Table II: Delay statistics and frame loss with different values of signal quality metrics in outdoor experiments.

Location	Avg. Delay (ms)									
	Min	Max	Mean	St.d.	Q1	Q3	Jitter	95% CI	Loss(%)	RSRP(dBm)
Loc 1	142.00	458.83	180.06	27.62	162.82	193.33	19.88	180.06 ± 0.44	1.52	-69.75
Loc 2	138.86	770.09	180.60	25.58	159.26	198.06	24.91	180.60 ± 0.41	0.01	-78.45
Loc 3	140.47	537.55	180.42	24.90	162.48	195.34	20.06	180.42 ± 0.40	1.20	-80.92
Loc 4	145.91	777.36	184.57	32.54	166.68	198.79	22.04	184.57 ± 0.52	1.27	-82.75
Loc 5	141.31	375.98	181.80	23.64	163.06	200.53	22.66	181.79 ± 0.38	0.22	-84.50
Loc 6	141.90	874.56	183.32	35.58	163.02	196.88	21.01	183.32 ± 0.57	1.40	-84.71
Loc 7	142.83	539.77	180.01	21.66	162.19	196.06	22.73	180.01 ± 0.35	0.16	-85.08
Loc 8	137.73	837.46	177.68	32.57	158.50	193.53	23.52	177.68 ± 0.52	0.01	-86.17
Loc 9	138.55	914.60	196.80	73.28	163.16	199.90	20.56	196.81 ± 1.18	0.26	-102.25

In Table II, we included network KPIs along with the average RSRP measured at each location in different experiments. In locations 2-8, the signal quality was in a similar RSRP range of around -80 dBm. The best signal (RSRP equal to -69.75 dBm) was measured in location 1, and the worst signal was in location 9, the furthest from the base station. The mean delay across all experiments was centered around 180 ms, except for location 9, where the lowest received power (RSRP equal to -102.25 dBm) was measured. The poor signal quality triggered more frequent retransmissions, causing a large delay of 196.80 ms. Interestingly, despite being close to the base station and registering a strong signal, location 1 did not perform better than other locations. Besides, the highest frame loss was observed at this location. This is because, despite the short distance from the base station, location 1 was surrounded by tall buildings. Therefore, despite the high received power at location 1, the LTE cat-M signal was intermittently available, leading to a frame loss (1.52%) higher than in other locations where the LTE cat-M signal was more reliable. In all other locations, the maximum measured frame loss was equal to 1.4%.

Jitter varied across the different locations within a relatively small range (19.88 ms to 24.91 ms), with the highest value measured at location 2. Delays in all locations were similarly distributed, as shown by the Q1 and Q3 values in Table II. Overall, these observations suggest that while RSRP is a valuable signal quality indicator that permits the study of the network's performance, there are other determining factors that may influence the network's actual performance. In particular, RSRP was measured through dedicated signal quality (SQ) frames transmitted from the smart grid nodes. However, these SQ frames could not be sent too often because they would drastically increase power consumption and overuse the limited available radio resources. The low rate at which signal quality was sampled did not permit capturing short signal degradations (as observed in location 1), leading to the discussed anomalies in the measured results.

C. Impact of the number of active nodes

In this study, we conducted outdoor experiments varying the number of active smart grid nodes from 1 to 8 to evaluate their impact on system performance. The resulting metrics, including mean delay, jitter, St.d., and frame loss at a transmission rate of $\lambda = 50$ fps, are averaged per experiment and presented in Table III.

Table III: Delay statistics and frame loss with varying number of active smart grid nodes in outdoor experiments.

No. of nodes	Avg. Delay (ms)								
	Min	Max	Mean	St.d.	Q1	Q3	Jitter	95% CI	Loss(%)
1	143.22	350.81	181.06	19.62	163.27	199.52	23.62	181.06 ± 0.32	1.11
2	143.94	461.60	181.92	20.08	163.82	197.24	22.82	181.93 ± 0.33	1.30
3	142.28	449.03	179.40	20.28	161.76	193.95	21.85	179.40 ± 0.32	1.06
4	141.79	541.78	181.13	22.64	163.29	195.31	20.80	181.13 ± 0.36	1.17
5	141.09	467.35	179.02	20.58	162.26	193.97	20.34	179.02 ± 0.33	1.04
6	142.52	460.90	179.65	20.76	162.98	192.67	20.00	179.65 ± 0.33	1.02
7	143.06	420.06	178.14	18.58	162.95	191.18	18.90	178.14 ± 0.30	1.00
8	141.73	403.58	177.29	19.77	162.10	189.76	18.44	177.29 ± 0.32	1.12

Our findings show that the mean delay remains relatively consistent, ranging from 177.29 to 181.93 ms, regardless of the number of active nodes. This consistency extends to the 95% CI, suggesting reliability in the measurements irrespective of node numbers. Interestingly, jitter values decrease as the number of nodes increases, from 23.62 ms with a single active node to 18.44 ms when eight nodes were deployed. However, the St.d. measurements show no clear trend with an increase in node count, suggesting that connecting up to 8 nodes to the same LTE cat-M base station doesn't significantly impact system performance. Moreover, the minimal variation in the overall frame loss rate underscores reliable network performance even with increased node counts.

D. Optimizing the transmission start time

According to 3GPP.36.331 E-UTRA standard [28], to initiate frame transmission over LTE-M, the User Equipment (UE) is required to send a scheduling request control message to the eNodeB and await a so-called scheduling grant (SG). SG contains information on time and frequency resources assigned to all nodes that transmit scheduling requests. SGs are periodically broadcasted with the system information (SI) control message, whose periodicity depends on the network

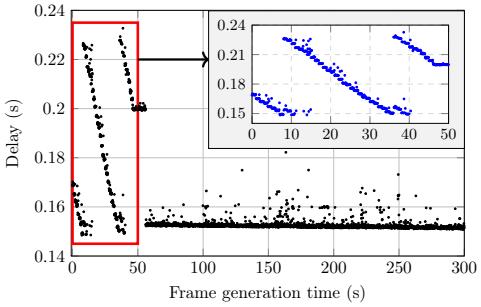

Figure 3: Delay with respect to the frame generation time in an experiment with λ = 12.5 fps.

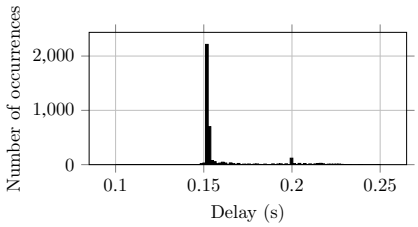

Figure 4: Histogram of the delays obtained with λ = 12.5 fps.

parameter *si-WindowLength-BR-r13*, which can range from 20 ms to 200 ms [28]. In the commercial LTE cat-M network used for our transmissions, this parameter equals 80 ms. In our previous work [9], we observed that most of the variability in the end-to-end delay is contributed by LTE cat-M radio access as other components, such as I2C or Internet-based delays, are considerably smaller and more stable. In particular, we observed the presence of a waiting time (between 0 and 80 ms) before the next SI message is transmitted. This led to a non-uniform packet inter-arrival time distribution for all rates except for λ = 12.5 fps, where packets were periodically spaced 80 ms apart, as the SI periodicity.

Leveraging this effect, we attempted to vary the transmission start time of smart grid nodes and analyze the impact on overall delay. To do so, we performed a so-called *calibration* for 50 s, during which we alternated a 1-second transmission period at 12.5 fps and a 2 ms pause. The server recorded the average delay received at each of these intervals. Then it determined the optimal transmission start time at the end of the calibration process and transmitted it to the smart grid nodes as a control message (see network architecture in Fig. 1). Performance results of this calibration technique are shown in Fig. 3. The red box highlights the *calibration process*, where we can observe *steps* in the delay over time. These steps have a width of 1 s (corresponding to the duration of the transmission interval) and a height of 2 ms due to a reduced waiting time, thanks to the delayed transmission. However, once the delay reaches a certain value (roughly 150 ms), the next step would result in an increased delay of 80 ms due to the waiting time of the next SI transmission. This technique, compared to a random transmission, can potentially reduce the average end-to-end delay of up to 80 ms. For example, in Fig. 3, we observe a maximum delay of 230 ms and a post-calibration delay of around 152 ms, which corresponds to a 33.91% reduction. The Probability Density Function (PDF) of the delay is also shown in Fig. 4, where it can be seen that the large majority of packets are received within 152 ms.

E. Analysis of different smart grid applications

In order to represent a wide variety of smart grid applications, we tested our multi-node testbed with a variable number of reporting rates. For instance, the C37.118.2-2011-IEEE Standard for Synchrophasor Data Transfer for Power Systems specifies the required reporting rate (for 50 Hz and 60 Hz power systems) as 10, 12, 15, 20, 25, 30, 50, and 60 fps depending on the application requirements (see Table 1 in [27]). In this work, we extended this range to 0.25-100 fps to further explore the suitability of LTE cat-M for other types of smart grid communications requiring smaller/higher reporting rates.

Table IV: Delay statistics Vs reporting rate.

Reporting rate λ fps	Avg. Delay (ms)								
	Min	Max	Mean	St.d.	Q1	Q3	Jitter	95% CI	Loss(%)
0.25	180.84	450.24	209.80	30.77	200.38	209.54	11.12	209.80 ± 4.05	1.56
0.5	194.24	261.43	212.52	06.02	209.21	215.09	1.98	212.52 ± 0.69	1.50
0.8	162.33	587.86	244.73	82.48	194.80	234.74	94.64	244.73 ± 7.42	1.04
1	164.48	411.83	211.25	63.15	171.68	211.38	66.33	211.25 ± 7.18	0.84
10	159.18	244.18	193.08	22.48	178.52	218.78	30.08	193.08 ± 0.81	1.06
20	151.43	361.68	186.66	20.02	173.28	204.32	29.90	186.66 ± 0.51	1.31
30	148.46	553.42	181.76	22.34	164.88	196.31	28.14	181.76 ± 0.46	1.20
50	142.00	423.57	180.68	19.87	162.89	195.85	21.34	180.68 ± 0.32	1.27
60	140.38	452.26	179.82	22.88	161.00	195.12	17.12	179.82 ± 0.33	1.29
80	141.34	674.53	179.76	27.95	160.06	194.02	13.62	179.76 ± 0.35	1.23
100	140.40	520.24	170.38	19.44	154.60	183.19	10.64	170.38 ± 0.22	1.17

The experiments were conducted outdoors for 5 minutes using two nodes, and the results were averaged for each reporting rate. Network KPIs, such as delay statistics, jitter, and frame loss, are included in Table IV. The first thing to remark is that low frame generation rates generally yield worse results with higher delay and larger jitter. In particular, when $\lambda \leq 1$ fps, the average delay is higher than 200 ms, whereas, at higher reporting rates, the average delay falls between 170 and 193 ms. Please note that this analysis did not use the calibration method explained in Section IV-D. It is also worth highlighting that the 95% CIs of the delay obtained with larger reporting rates are wider. From this result, we can infer that the variability of the delay at lower rates is larger.

These two effects, i.e., larger delays and 95% CIs at lower rates, can be explained by the fact that, with less frequent transmissions, the channel conditions can vary more significantly, leading to different transmission delays. For example, at 0.25 fps, two frames are spaced by 4 s, during which the propagation channel can vary with a remarkable effect on the measured delay. Conversely, at 100 fps, consecutive transmissions are 10 ms apart and are more likely to encounter similar propagating conditions, leading to similar delays. Moreover, when a device is idle for a long time, it may need to undergo random access more frequently, thus increasing the end-to-end delay. Frame loss maintains a consistent range between 0.84%

and 1.56% across all considered reporting rates, suggesting a modest influence of λ on the network performance.

V. Conclusion

This paper presents a multi-node testbed employing LTE cat-M technology to transmit packets from eight nodes to a control center. Nodes were deployed using simple off-the-shelf microcontrollers, i.e., Arduino DUE. Due to their design simplicity, these devices could be deployed on a larger scale and greatly benefit power utilities, researchers, and practitioners in the smart grid domain. An extensive network performance analysis has been conducted, based on KPIs such as delay and frame loss, to assess the suitability of this technology in the presence of smart grid traffic.

A wide variety of smart grid applications, represented by transmission rates ranging from 0.25 to 100 fps, were considered in this study and were used to prove the potential of LTE cat-M technology to serve smart grid traffic. A scalability analysis also proved that no significant performance degradation was observed when eight smart grid nodes simultaneously transmitted synchronous high-rate data. A comparison of the performance in indoor and outdoor scenarios was conducted to experimentally define the limits of LTE cat-M technology. An analysis of the impact of signal quality metrics, such as RSRP, on the network performance was also carried out, showing a limited effect of this parameter on the end-to-end delay.

Finally, a novel calibration method was presented to optimize the packet transmission start time, leveraging known properties of the LTE cat-M resource scheduling protocol. This calibration mechanism brought about a significant delay reduction, up to 33.91%, at a rate of 12.5 fps, and can be applied to other wireless technologies where radio resource scheduling is handled similarly, such as standard LTE or 5G.

References

[1] A. Usman and S. H. Shami, "Evolution of Communication Technologies for Smart Grid applications," *Renewable and Sustainable Energy Reviews*, vol. 19, pp. 191–199, 2013.

[2] B. Appasani and D. K. Mohanta, "A review on synchrophasor communication system: technologies, standards and applications," *Protection and control of modern power systems*, vol. 3, no. 1, pp. 1–17, 2018.

[3] B. Naduvathuparambil, M. Valenti, and A. Feliachi, "Communication delays in wide area measurement systems," in *Proceedings of the Thirty-Fourth Southeastern Symposium on System Theory (Cat. No.02EX540)*, 2002, pp. 118–122.

[4] P. Rengaraju, C.-H. Lung, and A. Srinivasan, "Communication requirements and analysis of distribution networks using WiMAX technology for smart grids," in *2012 8th International Wireless Communications and Mobile Computing Conference (IWCMC)*, 2012, pp. 666–670.

[5] A. Borghetti, R. Bottura, M. Barbiroli, and C. A. Nucci, "Synchrophasors-Based Distributed Secondary Voltage/VAR Control via Cellular Network," *IEEE Transactions on Smart Grid*, vol. 8, no. 1, pp. 262–274, 2017.

[6] A. Derviškadić, P. Romano, M. Pignati, and M. Paolone, "Architecture and Experimental Validation of a Low-Latency Phasor Data Concentrator," *IEEE Transactions on Smart Grid*, vol. 9, no. 4, pp. 2885–2893, 2018.

[7] F. Malandra, R. Pourramezan, H. Karimi, and B. Sansò, "Impact of PMU and Smart Meter Applications on the Performance of LTE-based Smart City Communications," in *2018 IEEE 29th Annual International Symposium on Personal, Indoor and Mobile Radio Communications (PIMRC)*, 2018, pp. 1–6.

[8] N. Accurso, N. Mastronarde, and F. Malandra, "Exploring Tradeoffs between Energy Consumption and Network Performance in Cellular-IoT: a Survey," in *2021 IEEE Global Communications Conference (GLOBECOM)*, 2021, pp. 01–06.

[9] S. Shah, S. Koley, and F. Malandra, "Experimental End-To-End Delay Analysis of LTE cat-M With High-Rate Synchrophasor Communications," *IEEE Internet of Things Journal*, pp. 1–1, 2023.

[10] I. Srivastava, S. Bhat, and A. R. Singh, "Smart Grid Communication: Recent Trends and Challenges," *Next Generation Smart Grids: Modeling, Control and Optimization*, pp. 49–75, 2022.

[11] N. Suhaimy, N. A. M. Radzi, W. S. H. M. W. Ahmad, K. H. M. Azmi, and M. A. Hannan, "Current and Future Communication Solutions for Smart Grids: A Review," *IEEE Access*, vol. 10, pp. 43 639–43 668, 2022.

[12] T. Docquier, Y.-Q. Song, V. Chevrier, L. Pontnau, and A. Ahmed-Nacer, "Performance evaluation methodologies for Smart Grid Substation Communication Networks: A survey," *Computer Communications*, 2022.

[13] F. Malandra and B. Sanso, "A Simulation Tool for the Performance Evaluation of Large-scale RF-Mesh Networks for Smart Grid and IoT Applications," in *The 1st EAI International Conference on Smart Grid Assisted Internet of Things*, 2017, pp. 54–63.

[14] Y. Seyedi, H. Karimi, F. Malandra, B. Sansò, and J. Mahseredjian, "Coordinated Control of Distributed Energy Resources Using Features of Voltage Disturbances," *IEEE Transactions on Industrial Informatics*, vol. 16, no. 6, pp. 3895–3904, 2020.

[15] W. K. Chai, N. Wang, K. V. Katsaros, G. Kamel, G. Pavlou, S. Melis, M. Hoefling, B. Vieira, P. Romano, S. Sarri, T. T. Tesfay, B. Yang, F. Heimgaertner, M. Pignati, M. Paolone, M. Menth, E. Poll, M. Mampaey, H. H. I. Bontius, and C. Develder, "An Information-Centric Communication Infrastructure for Real-Time State Estimation of Active Distribution Networks," *IEEE Transactions on Smart Grid*, vol. 6, no. 4, pp. 2134–2146, 2015.

[16] G. Bumiller, L. Lampe, and H. Hrasnica, "Power line communication networks for large-scale control and automation systems," *IEEE Communications Magazine*, vol. 48, no. 4, pp. 106–113, 2010.

[17] H. Gharavi and B. Hu, "Scalable Synchrophasors Communication Network Design and Implementation for Real-Time Distributed Generation Grid," *IEEE Transactions on Smart Grid*, vol. 6, no. 5, pp. 2539–2550, 2015.

[18] Q. Wang, Y. Lin, and H. Zhan, "A hybrid wireless system for power line monitoring," in *IEEE PES Innovative Smart Grid Technologies*, 2012, pp. 1–6.

[19] F. Malandra, S. Rochefort, P. Potvin, and B. Sansò, "A case study for M2M traffic characterization in a smart city environment," in *Proceedings of the 1st International Conference on Internet of Things and Machine Learning*, 2017, pp. 1–9.

[20] F. Malandra, L.-O. Chiquette, L.-P. Lafontaine-Bédard, and B. Sansò, "Traffic characterization and LTE performance analysis for M2M communications in smart cities," *Pervasive and Mobile Computing*, vol. 48, pp. 59–68, 2018.

[21] M.-S. Kang, Y.-L. Ke, and J.-S. Li, "Implementation of smart loading monitoring and control system with ZigBee wireless network," in *6th IEEE Conf. on Industrial Electronics and Applic.*, 2011, pp. 907–912.

[22] A. Meloni, P. A. Pegoraro, L. Atzori, P. Castello, and S. Sulis, "IoT cloud-based distribution system state estimation: Virtual objects and context-awareness," in *2016 IEEE International Conference on Communications (ICC)*, 2016, pp. 1–6.

[23] R. Samoilenko, N. Accurso, and F. Malandra, "A Simulation Study on the Impact of IoT Traffic in a Smart-city LTE Network," in *2020 IEEE 31st Annual International Symposium on Personal, Indoor and Mobile Radio Communications*, 2020, pp. 1–6.

[24] B. K. Dash and J. Peng, "Zigbee Wireless Sensor Networks: Performance Study in an Apartment-Based Indoor Environment," *Journal of Computer Networks and Communications*, vol. 2022, 2022.

[25] P.-C. Hsieh, Y. Jia, D. Parra, and P. Aithal, "An Experimental Study on Coverage Enhancement of LTE Cat-M1 for Machine-Type Communication," in *2018 IEEE International Conference on Communications (ICC)*, 2018, pp. 1–5.

[26] M. Elsaadany, A. Ali, and W. Hamouda, "Cellular LTE-A Technologies for the Future Internet-of-Things: Physical Layer Features and Challenges," *IEEE Communications Surveys & Tutorials*, vol. 19, no. 4, pp. 2544–2572, 2017.

[27] "IEEE Standard for Synchrophasor Data Transfer for Power Systems," *IEEE Std C37.118.2-2011 (Revision of IEEE Std C37.118-2005)*, pp. 1–53, 2011.

[28] 3GPP, "Evolved Universal Terrestrial Radio Access (E-UTRA);Radio Resource Control(RRC);Protocol specification," 3rd Generation Partnership Project (3GPP), Technical specification(TS) 36.331, 2020, version 15.10.0. [Online]. Available: https://portal.3gpp.org/desktopmodules/Specifications/SpecificationDetails.aspx?specificationId=2440